



**HAL**  
open science

## Strain mapping of tensile strained silicon transistors with embedded Si<sub>1-y</sub>C<sub>y</sub> source and drain by dark-field holography

Florian Hue, Martin Hytch, Florent Houdellier, Hugo Bender, Alain Claverie

### ► To cite this version:

Florian Hue, Martin Hytch, Florent Houdellier, Hugo Bender, Alain Claverie. Strain mapping of tensile strained silicon transistors with embedded Si<sub>1-y</sub>C<sub>y</sub> source and drain by dark-field holography. Applied Physics Letters, 2009, 95 (7), pp.73103 - 73103. 10.1063/1.3192356 . hal-01742020

**HAL Id: hal-01742020**

**<https://hal.science/hal-01742020v1>**

Submitted on 27 Mar 2018

**HAL** is a multi-disciplinary open access archive for the deposit and dissemination of scientific research documents, whether they are published or not. The documents may come from teaching and research institutions in France or abroad, or from public or private research centers.

L'archive ouverte pluridisciplinaire **HAL**, est destinee au depot et a la diffusion de documents scientifiques de niveau recherche, publies ou non, emanant des tablissements d'enseignement et de recherche franais ou trangers, des laboratoires publics ou privs.

# Strain mapping of tensile strained silicon transistors with embedded $\text{Si}_{1-y}\text{C}_y$ source and drain by dark-field holography

Florian He, Martin Htch, Florent Houdellier, Hugo Bender, and Alain Claverie

Citation: *Appl. Phys. Lett.* **95**, 073103 (2009); doi: 10.1063/1.3192356

View online: <https://doi.org/10.1063/1.3192356>

View Table of Contents: <http://aip.scitation.org/toc/apl/95/7>

Published by the [American Institute of Physics](#)

---

## Articles you may be interested in

[Improved precision in strain measurement using nanobeam electron diffraction](#)

*Applied Physics Letters* **95**, 123114 (2009); 10.1063/1.3224886

[Dark field electron holography for quantitative strain measurements with nanometer-scale spatial resolution](#)

*Applied Physics Letters* **95**, 053501 (2009); 10.1063/1.3196549

[On the influence of elastic strain on the accommodation of carbon atoms into substitutional sites in strained Si:C layers grown on Si substrates](#)

*Applied Physics Letters* **94**, 141910 (2009); 10.1063/1.3116648

[Measurement of incomplete strain relaxation in a silicon heteroepitaxial film by geometrical phase analysis in the transmission electron microscope](#)

*Applied Physics Letters* **91**, 231902 (2007); 10.1063/1.2821843

[The addition of strain in uniaxially strained transistors by both SiN contact etch stop layers and recessed SiGe sources and drains](#)

*Journal of Applied Physics* **112**, 094314 (2012); 10.1063/1.4764045

[An efficient, simple, and precise way to map strain with nanometer resolution in semiconductor devices](#)

*Applied Physics Letters* **96**, 091901 (2010); 10.1063/1.3337090

---

**Scilight**

Sharp, quick summaries **illuminating**  
the latest physics research

Sign up for **FREE!**

**AIP**  
Publishing

# Strain mapping of tensile strained silicon transistors with embedded $\text{Si}_{1-y}\text{C}_y$ source and drain by dark-field holography

Florian Hue,<sup>1,a)</sup> Martin Hytch,<sup>1</sup> Florent Houdellier,<sup>1</sup> Hugo Bender,<sup>2</sup> and Alain Claverie<sup>1</sup>

<sup>1</sup>CNRS, CEMES, 29 rue Jeanne Marvig, F-31055 Toulouse, France and Universite de Toulouse,

UPS, F-31055 Toulouse, France

<sup>2</sup>IMEC, Kapeldreef 75, 3001 Leuven, Belgium

(Received 5 June 2009; accepted 9 July 2009; published online 18 August 2009)

Dark-field holography, a new transmission electron microscopy technique for mapping strain distributions at the nanoscale, is used to characterize strained-silicon *n*-type transistors with a channel width of 65 nm. The strain in the channel region, which enhances electron mobilities, is engineered by recessed  $\text{Si}_{0.99}\text{C}_{0.01}$  source and drain stressors. The strain distribution is measured across an array of five transistors over a total area of 1.6  $\mu\text{m}$  wide. The longitudinal tensile strain reaches a maximum of  $0.58\% \pm 0.02\%$  under the gate oxide. Theoretical strain maps obtained by finite element method agree well with the experimental results. © 2009 American Institute of Physics. [DOI: 10.1063/1.3192356]

Strained-silicon channel technology is now implemented in all the latest generation of nanoelectronic devices.<sup>1,2</sup> Straining silicon considerably increases the mobility of carriers, either electrons or holes, leading to significantly enhanced performances in metal-oxide-semiconductor field-effect transistors (MOSFETs).<sup>3-5</sup> Different techniques have been investigated to engineer strain in devices, for example the growth of relaxed virtual substrates to induce biaxial strain in the channel region, or the capping of transistors with a specially engineered high tensile stress silicon nitride layer to induce uniaxial tensile strain.<sup>6,7</sup> The most widely reported technique, however, is to use recessed  $\text{Si}_{1-x}\text{Ge}_x$  or  $\text{Si}_{1-y}\text{C}_y$  sources and drains as stressors for compressive strain in *p*-MOSFETs<sup>8</sup> and tensile strain in *n*-MOSFETs,<sup>9,10</sup> respectively. By combining these different methods, it is possible to induce various distributions of strain.<sup>11</sup> Nevertheless, detailed knowledge of the exact strain distribution in two dimensions is required to understand how improvements in performance can be optimized.

Transmission electron microscopy (TEM) is the most appropriate tool for measuring strains at the nanoscale. Convergent-beam electron diffraction<sup>12-14</sup> and nanobeam diffraction<sup>15</sup> can be used to measure strain accurately at specific points on the sample but are less suited for the mapping of strains continuously across devices. More recently, aberration-corrected high-resolution transmission electron microscopy (HRTEM)<sup>16</sup> has been used to map strains in *p*-MOSFET devices. Nevertheless, the method, although promising, suffers from the limited field of view, sample preparation issues, and the inherently low signal-to-noise ratio of HRTEM observations. To overcome these difficulties, we recently introduced an electron holographic technique for measuring strain (HoloDark).<sup>17,18</sup> The technique is based on the interference of diffracted beams from adjacent sample areas using the dark-field holography configuration.<sup>19</sup> Unlike conventional off-axis holography, the phase differences in

the diffracted beams give direct access to local changes in the lattice parameters.<sup>17</sup>

In this paper, we report on the analysis by dark-field holography of the strain distribution in *n*-MOSFETs with recessed sources and drains of carbon-doped silicon. The measurement of strain in such devices<sup>10,20,21</sup> is more challenging than for SiGe/Si systems, as the lattice mismatches are significantly smaller. We will also demonstrate a recent improvement in the precision and field of view of the technique.

A series of dummy transistors with a channel width of 65 nm were prepared using  $\text{Si}_{0.99}\text{C}_{0.01}$  sources and drains stressors for the Si channel in an ASM Epsilon<sup>®</sup> 2000 reactor.<sup>22</sup> TEM samples were prepared by focus ion beam for  $[1\bar{1}0]$  zone axis observations [Fig. 1(a)] to a thickness of about 150 nm. The optimized preparation method maintains a relatively thick region of substrate adjacent to the thinned outer edge and prevents the specimen from bowing and cracking.

Microscope observations were performed on the SACTEM-Toulouse, a Tecnai F20 (FEI) TEM operating at

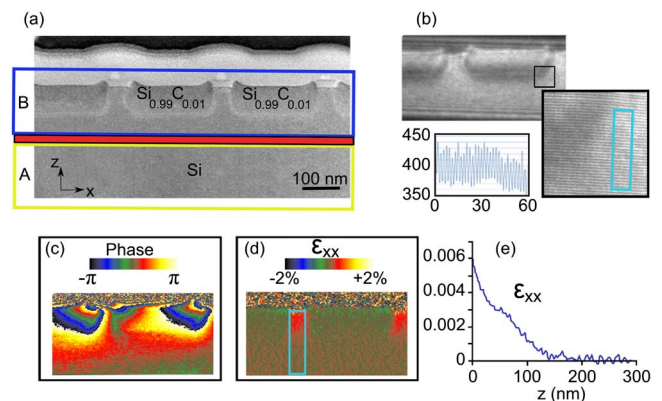


FIG. 1. (Color online) Dark-field strain analysis of *n*-MOSFETs with embedded  $\text{Si}_{0.99}\text{C}_{0.01}$  sources and drains: (a) conventional TEM observation of the structure, (b) dark-field hologram obtained by interfering the (220) diffracted beams from areas A and B, (c) phase analysis of hologram revealing local changes of lattice parameter, and (d)  $\epsilon_{xx}$  strain map with profile in channel from gate oxide to substrate (e). A maximum tensile deformation occurs close to the gate.

<sup>a)</sup>Present address: Department of Materials Science and Metallurgy, University of Cambridge, Pembroke Street, Cambridge CB2 3QZ, United Kingdom. Electronic mail: fmh29@cam.ac.uk.

200 kV, equipped with field-emission gun, electrostatic biprism, and imaging aberration corrector (CEOS). Holograms were recorded on a  $2048 \times 2048$  pixel charge-coupled device (CCD) camera (Gatan USC1000). The first transfer lens of the corrector was used as a Lorentz lens<sup>23,24</sup> with the objective lens switched off. In this configuration, fields of view are wider and the overlap area of the hologram can easily reach 300 nm (relative to the specimen) with biprism voltages of about 100 V. Typical contrasts for 2 nm fringes were 13% for a 4-s exposure time [Fig. 1(b)]. Dark-field holography was performed with different diffracted beams: (111),  $(\bar{1}\bar{1}\bar{1})$ , (002), and (220). Images were corrected for the geometric distortions introduced by the CCD camera. Hologram analysis was carried out using in-house software and GPA PHASE 2.0 (HREM Research), a plug-in for the DIGITALMICROGRAPH image processing package (Gatan). The Fourier space mask used in the analysis limits our spatial resolution of strain measurements to 4 nm. Strain modeling was carried out using the software package COMSOL MULTIPHYSICS.

The longitudinal strain in the  $x$  direction, parallel to the gate, can be measured from the phase of a single diffracted component in the  $x$  direction (220, 440,...) or from a combination of phases from two noncollinear diffracted beams. The former method has the advantage of speed and simplicity but the latter is necessary to access the full two-dimensional (2D) strain tensor. Figure 1(b) shows an experimental dark-field hologram obtained from the (220) diffracted beam. The biprism is placed 300 nm (relative to the object plane) under the gate and parallel to the surface in order to interfere the diffracted wave from the Si substrate with the diffracted wave from the strained area of the MOSFET. Ideally, the measurement area should contain part of the substrate to be able to define the carrier frequency. The phase of the holographic fringes, Fig. 1(c), depends on the local difference in the lattice parameter between the substrate and the area of interest. The local deformation is calculated from the phase gradients in the framework of geometric phase analysis (GPA).<sup>25</sup>

Errors are introduced if phase terms from the mean-inner potential or dynamic scattering within the specimen vary across the field of view. Such variations can be limited by accurately controlling the specimen thickness and avoiding specimen bending, which would change the local diffraction conditions and hence the dynamical phase. These conditions can be verified experimentally by observing that the intensity of the dark-field image is uniform in the region analyzed. Inevitably the mean-inner potential will be different in the Si:C layer and the silicon substrate. However, the difference is extremely small and will only produce a phase gradient at the interfaces.

Figure 1(d) presents a map of the longitudinal strain. Doping the silicon with carbon (nominally to 1%) reduces the lattice parameter of the source and drain area, which in turn stretches the channel in the  $x$  direction. The tensile strain reaches a maximum of 0.6% near the gate oxide and decreases progressively toward the bulk. After twice the distance of the source and drain depth, the stressors have no more influence on the strain and the crystal recovers its bulk lattice parameter.

Dark-field holography can be used in this configuration to measure strains over a relatively wide field of view (up to

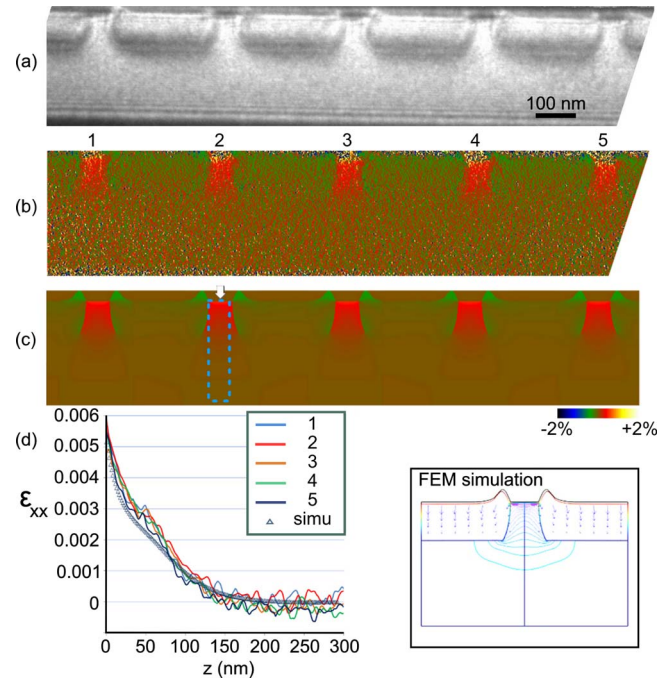


FIG. 2. (Color online) Dark-field hologram analysis of transistor array: (a) dark-field hologram with the (220) diffracted beam, (b) corresponding  $\epsilon_{xx}$  strain map relative to Si substrate, (c) FEM simulation, and (d) strain profiles from five different channels from gate oxide to substrate. Maximum strain under the gate is  $0.58\% \pm 0.02\%$ .

$300 \times 800 \text{ nm}^2$ ) but this can be enlarged by modifying the projector lenses system. Figure 2(a) shows the widest observation that we have been able to obtain on the SACTEM with an acceleration voltage of 200 kV. The limit is determined by the size of the CCD camera, and in particular, the Nyquist frequency limit for the holographic fringes. The exposure time is 10 s and the fringes period is only 2.5 pixels. Although contrast and precision are reduced, the field of view has been doubled ( $1.6 \mu\text{m}$ ). The overlap itself is unchanged as this depends on the biprism voltage.

It is now possible to map the deformation field in five different transistor channels in just one acquisition, which ensures that the reference is exactly the same for each transistor and allows a statistical analysis of the measured strain distributions. Figure 2(d) shows the profiles taken in each separate channel from the gate to the substrate. The width of integration corresponds to the length of the channels: 65 nm. There is an excellent agreement between all of the measured profiles, with each curve following exactly the same trend, including the slight deviation about 65 nm from the gate. Indeed, the standard deviation between the profiles is only 0.02%, which expresses the precision of our measurements. The maximum value, just below the gate, is  $0.58\% \pm 0.02\%$ , which suggests that the reduced sampling has not introduced a significant systematic error.

To estimate the accuracy of the method we have realized a finite element method (FEM) model based on linear elasticity theory.<sup>26,16</sup> Initially, we performed full three-dimensional simulations (150 nm thick) with free surfaces and a geometry that mimics that one revealed by TEM bright-field images [Fig. 1(a)]. The results show no significant thin foil relaxation, mainly due to the large thickness and the specific geometry of the specimen. To simplify subsequent calculations, we therefore turned to a 2D plane-strain

model which is sufficient for our purposes. The surfaces of the TEM lamella are considered to be rigid and only the upper surface (in the  $z$  direction), near the oxide, is free.

The two following subdomains are considered: one with Si properties (bulk elastic constants and lattice parameter) and another with  $\text{Si}_{1-y}\text{C}_y$  properties. The nominal value of  $y$  is 1% but not all carbon atoms are incorporated on substitutional sites, and thus contribute to the modification of the lattice parameter.<sup>27,28</sup> From  $\mu$ -Raman experiments on uniform layers we can estimate that only between 75% (Ref. 29) and 90% (Ref. 22) of carbon atoms are involved in the strain process. Figure 2(c) shows the results from the best fitting FEM model with  $y=0.75\%$ , a mesh step of 4 nm and identical color scale to the experimental results in Figs. 2(b) and 1(d). We have confirmed the value of 0.75% for the substitutional carbon by analyzing the lattice parameter in the Si:C layer in the  $z$  direction with a (002) dark-field hologram.

The simulated profile of  $\varepsilon_{xx}$  follows closely the trend of the experimental results [Fig. 2(d)]. The standard deviation between the average of the experimental profiles and the simulation is only 0.01%, although a systematic difference of 0.04% occurs nearer the gate. This is reflected in the maximum reached by the simulation, 0.53%, compared with the experiment value of 0.58%. The underestimation of the strain by the model is probably due to the difficulty of reproducing exactly the same boundary conditions, such as the effect of the top oxide, or the gate and the surface platinum layer.

We have demonstrated that dark-field holography is a valuable tool for the study of strained-silicon  $n$ -MOSFETs where strains tend to be relatively small and highly localized. Strain can be measured to extremely high precision ( $2 \cdot 10^{-4}$ ) and mapped across large field of view (300 nm by 1.6  $\mu\text{m}$ ) with good spatial resolution (4 nm). By studying five neighboring transistors, information of a statistical nature can be obtained. The Si channels have a longitudinal strain  $\varepsilon_{xx}$  which is maximal near the gate oxide at a value of  $0.58\% \pm 0.02\%$  before decreasing progressively toward the substrate. The FEM modeling shows that the results are consistent with a substitutional carbon content in the recessed sources and drains of 0.75% of the total carbon concentration.

This work was supported by the European Commission through the ESTEEM project (Enabling Science and Technology for European Electron Microscopy, Grant No. IP3: 0260019), the French Government (MINEFI) through the NANO2012 initiative (project IMASTRAIN), and by the French National Agency (ANR) in the frame of its program in Nanosciences and Nanotechnologies (HD STRAIN Project No. ANR-08-NANO-0 32). Peter Verheyen and Roger Loo (IMEC) are gratefully acknowledged for supplying the device material.

<sup>1</sup>The International Technology Roadmap for Semiconductors, Edition 2007, Process Integration, Devices & Structures.

- <sup>2</sup>M. L. Lee, E. A. Fitzgerald, M. T. Bulsara, M. T. Currie, and A. Lochtefeld, *J. Appl. Phys.* **97**, 011101 (2005).
- <sup>3</sup>E. A. Fitzgerald, *Mater. Sci. Eng., B* **124**, 8 (2005).
- <sup>4</sup>S. E. Thompson, G. Sun, Y. S. Choi, and T. Nishida, *IEEE Trans. Electron Devices* **53**, 1010 (2006).
- <sup>5</sup>D. A. Antoniadis, I. Aberg, C. Ni Chleirigh, O. M. Nayfeh, A. Khakifirooz, and J. L. Hoyt, *IBM J. Res. Dev.* **50**, 363 (2006).
- <sup>6</sup>S. Ito, H. Namba, T. Hirata, K. Ando, S. Koyama, N. Ikezawa, T. Suzuki, T. Saitoh, and T. Horiuchi, *Microelectron. Reliab.* **42**, 201 (2002).
- <sup>7</sup>C. H. Chen, T. L. Lee, T. H. Hou, C. L. Chen, C. C. Chen, J. W. Hsu, K. L. Cheng, Y. H. Chiu, H. J. Tao, Y. Jin, C. H. Diaz, S. C. Chen, and M. S. Liang, *Dig. Tech. Pap. - Symp. VLSI Technol.* **2004**, 56.
- <sup>8</sup>G. Eneman, P. Verheyen, R. Rooyackers, F. Nouri, L. Washington, R. Schreutelkamp, V. Moroz, L. Smith, A. De Keersgieter, M. Jurczak, and K. De Meyer, *IEEE Trans. Electron Devices*, **53**, 1647 (2006).
- <sup>9</sup>Y. Liu, O. Gluschenkov, J. Li, A. Madan, A. Ozcan, B. Kim, T. Dyer, A. Chakravarti, K. Chan, C. Lavoie, I. Popova, T. Pinto, N. Rovedo, Z. Luo, R. Loesing, W. Henson, and K. Rim, *Dig. Tech. Pap. - Symp. VLSI Technol.* **2007**, 44.
- <sup>10</sup>C. J. Chui, K. W. Ang, N. Balasubramanian, M. F. Li, G. S. Samudra, and Y. C. Yeo, *IEEE Trans. Electron Devices* **54**, 249 (2007).
- <sup>11</sup>K. W. Ang, J. Lin, C. H. Tung, N. Balasubramanian, G. Samudra, and Y. C. Yeo, *Dig. Tech. Pap. - Symp. VLSI Technol.* **2007**, 42.
- <sup>12</sup>J. Huang, M. J. Kim, P. R. Chidambaram, R. B. Irwin, P. J. Jones, J. W. Weijtmans, E. M. Koontz, Y. G. Wang, S. Tang, and R. Wise, *Appl. Phys. Lett.* **89**, 063114 (2006).
- <sup>13</sup>P. Zhang, A. A. Istratov, E. R. Weber, C. Kisielowski, H. F. He, C. Nelson, and J. C. H. Spence, *Appl. Phys. Lett.* **89**, 161907 (2006).
- <sup>14</sup>W. Zhao, G. Duscher, G. Rozgonyi, M. A. Zikry, S. Chopra, and M. C. Ozturk, *Appl. Phys. Lett.* **90**, 191907 (2007).
- <sup>15</sup>K. Usada, Y. Numata, T. Irisawa, N. Hirashita, and S. Takegi, *Mater. Sci. Eng., B* **124-125**, 143 (2005).
- <sup>16</sup>F. Hüe, M. J. Hÿtch, F. Houdellier, J. M. Hartmann, H. Bender, and A. Claverie, *Phys. Rev. Lett.* **100**, 156602 (2008).
- <sup>17</sup>M. J. Hÿtch, F. Houdellier, F. Hüe, and E. Snoeck, *Nature (London)* **453**, 1086 (2008).
- <sup>18</sup>M. J. Hÿtch, F. Houdellier, F. Hüe, and E. Snoeck, Patent Application No. FR 07 06711 (pending).
- <sup>19</sup>K. J. Hanszen, *J. Phys. D* **19**, 373 (1986).
- <sup>20</sup>P. Favia, D. Klenov, G. Eneman, P. Verheyen, M. Bauer, D. Weeks, S. G. Thomas, and H. Bender, in *Strain Study in Transistors with SiC and SiGe Source and Drain by STEM Nano Beam Diffraction*, edited by S. Richter and A. Schwedt (EMC, Springer Berlin Heidelberg, 2009) Vol. 2, pp. 15–16.
- <sup>21</sup>H. Itokawa, N. Yasutake, N. Kusunoki, S. Okamoto, N. Aoki, and I. Mizushima, *Appl. Surf. Sci.* **254**, 6135 (2008).
- <sup>22</sup>P. Verheyen, V. Machkaoutsan, M. Bauer, D. Weeks, C. Kerner, F. Clemente, H. Bender, D. Shamiryan, R. Loo, T. Hoffmann, P. Absil, S. Biesemans, and S. G. Thomas, *IEEE Electron Device Lett.* **29**, 1206 (2008).
- <sup>23</sup>E. Snoeck, P. Hartel, H. Mueller, M. Haider and P. C. Tiemeijer, *Proceedings of the International Microscopic Conference (IMC 16, Sapporo, 2006)* Vol. 2, p. 730.
- <sup>24</sup>F. Houdellier, M. J. Hÿtch, F. Hüe, and E. Snoeck, *Advances in Imaging and Electron Physics*, edited by P. W. Hawkes (Elsevier, Amsterdam, 2008), Vol. 153, Chap. 6, pp. 1–36.
- <sup>25</sup>M. J. Hÿtch, E. Snoeck, and R. Kilaas, *Ultramicroscopy* **74**, 131 (1998).
- <sup>26</sup>Y. C. Yeo and J. S. Sun, *Appl. Phys. Lett.* **86**, 023103 (2005).
- <sup>27</sup>J. M. Hartmann, T. Ernst, V. Loup, F. Ducroquet, G. Rolland, D. Lafond, P. Holliger, F. Laugier, M. N. Séméria, and S. Deleonibus, *J. Appl. Phys.* **92**, 2368 (2002).
- <sup>28</sup>V. Le Thanh, C. Calmes, Y. Zheng, and D. Bouchier, *Appl. Phys. Lett.* **80**, 43 (2002).
- <sup>29</sup>N. Cherkashin, M. J. Hÿtch, F. Houdellier, F. Hüe, V. Paillard, A. Claverie, A. Gouyé, O. Kermaec, D. Rouchon, M. Burdin, and P. Holliger, *Appl. Phys. Lett.* **94**, 141910 (2009).